Depolarization field of spheroidal particles

Alexander Moroz

Wave-scattering.com (wavescattering@yahoo.com)

Received October 21, 2008; accepted November 30, 2008;
posted December 18, 2008 (Doc. ID 103068); published February 24, 2009

A compact analytical formula up to the order of k^3, where k is a wave vector, is derived for the depolarization field $\mathbf{E}_d$ of a spheroidal particle by performing explicitly the steps of the recipe outlined by Meier and Wokaun [Opt. Lett. **8**, 581 (1983)]. For the static component of $\mathbf{E}_d$ a general electrostatic formula valid for a particle of a general shape is rederived within the Meier and Wokaun framework. The dynamic k^2-dependent depolarization component of $\mathbf{E}_d$ is shown to depend on *dynamic* geometrical factors, which can be expressed in terms of the standard geometrical factors of electrostatics. The Meier and Wokaun recipe itself is shown to be equivalent to a long-wavelength limit of the Green's function technique. The resulting Meier and Wokaun long-wavelength approximation is found to exhibit a redshift compared against exact T-matrix results. At least for a sphere, it is possible to get rid of the redshift by assuming a weak nonuniformity of the field $\mathbf{E}_{int}$ inside a particle, which can be fully accounted for by a renormalization of the dynamic geometrical factors. My results may be relevant for various plasmonic, or nanoantenna, applications of spheroidal particles with a dominant electric dipole scattering, whenever it is necessary to go beyond the Rayleigh approximation and to capture the essential size-dependent features of scattering, local fields, SERS, hyper-Raman and second-harmonic-generation enhancements, decay rates, and photophysics of dipolar arrays.

OCIS codes: 350.4238, 290.3770, 240.6680, 250.5403.

1. INTRODUCTION

An ongoing development in plasmonic applications of small metal particles in biology, energy conversion, medicine, sensing, and many other fields requires a reliable description of electromagnetic fields inside, in close proximity to, or far away from particles of a general shape, which can be readily obtained by current experimental techniques [1,2]. It goes without saying that size provides important control over many of the physical and chemical properties of nanoscale materials. The focus of the present paper is on particles for which the electric dipole scattering is the dominant one, yet the Rayleigh limit is insufficient in capturing their essential size-dependent features exhibited in the behavior of their cross sections and local field enhancements [3], and in the redshift of the surface plasmon resonance (SPR) (Section 12.1.1. of [4]). The above range corresponds essentially to nanoparticles with a volume equivalent to that of a sphere with the radius between 5 and ≈50 nm in the visible [3,5–11]. In spite of a number of numerical methods for metal particles, such as discrete dipole approximation (DDA) [8–11], the method of moments [12], and the T-matrix method [13–17], it is insightful to understand the main features of electromagnetic fields around small particles in simpler intuitive terms. This is often achieved by approximating a small particle by an appropriate ellipsoidally shaped particle. The latter is possible for a wide range of shapes, ranging from a rodlike to disklike shaped particles. Ellipsoidal particles are also interesting on their own and have been studied in connection with a size dependence of surface-enhanced Raman scattering (SERS) and hyper-Raman enhancements [8–11]. For a small ellipsoidal particle, the internal field inside a particle $\mathbf{E}_{int}$ can be assumed to a high degree to be *homogeneous*. Indeed, according to the recently proved *weak Eshelby conjecture* [18] applied to electrostatics, if a particle is of elliptic or ellipsoidal in shape, then for any *uniform* applied field $\mathbf{E}_0$ the field $\mathbf{E}_{int}$ inside the particle is *uniform*. The converse is also true, i.e., that if the field inside a particle is *uniform* for all uniform applied fields, then the particle is of elliptic or ellipsoidal shape. (In two dimensions, the so-called *strong Eshelby conjecture* applies: if the field inside a particle is uniform for a single uniform applied field, then the particle is of elliptic shape [18].) A key issue in describing the optical properties of small particles is a proportionality relation between the homogeneous fields $\mathbf{E}_0$ and $\mathbf{E}_{int}$. In classical electrodynamics one can write $\mathbf{E}_{int}$ as

$$\mathbf{E}_{int} = \mathbf{E}_0 + \mathbf{E}_d, \tag{1}$$

where $\mathbf{E}_d$ stands for a *depolarization field* [19].

Let V be the particle volume; ε_p be the particle dielectric constant; ε_h be the dielectric constant of a surrounding host medium; $\varepsilon = \varepsilon_p/\varepsilon_h$; and $k = 2\pi\sqrt{\varepsilon_h}/\lambda$, where λ is the vacuum wavelength, be the wave vector in the surrounding medium. A great deal of insight has been achieved by the work of Meier and Wokaun [3], who suggested that the depolarization field $\mathbf{E}_d$ generated by the polarized matter surrounding the center of the sphere can be determined in the following steps:

1. Assigning a dipole moment $d\mathbf{p}(\mathbf{r}) = (\mathbf{P}/\varepsilon_h)dV$, with $\mathbf{P}$ denoting polarization, to each volume element dV of a particle,
2. calculating the retarded dipolar field $d\mathbf{E}_d$ generated by $d\mathbf{p}(\mathbf{r})$ at the center, and

3. integrating $d\mathbf{E}_d$ over the volume of a sphere.

After performing the above steps for a sphere of radius a [3],

$$\mathbf{E}_d = -\frac{4\pi}{3\varepsilon_h}\left(1 - x^2 - i\frac{2}{3}x^3\right)\mathbf{P}, \tag{2}$$

where $x=ka$ stands for the conventional size parameter [4]. After substituting the result back into the defining equation for a polarization $\mathbf{P}$,

$$4\pi\mathbf{P} = \varepsilon_h(\varepsilon - 1)\mathbf{E}_{int} = \varepsilon_h(\varepsilon - 1)(\mathbf{E}_0 + \mathbf{E}_d), \tag{3}$$

the following polarizability (defined via $\mathbf{d}=\varepsilon_h\alpha\mathbf{E}_0$, where $\mathbf{d}=\frac{4}{3}\pi a^3\mathbf{P}$ is the induced dipole moment) results:

$$\alpha_{MW} = \frac{\varepsilon - 1}{\varepsilon + 2 - (\varepsilon - 1)x^2 - i\dfrac{2x^3}{3}(\varepsilon - 1)}a^3. \tag{4}$$

The k^2-dependent term in the denominator ($x=ka$) is usually called a *dynamic depolarization* and has been interpreted as arising from a dephasing between radiation emitted by different parts of the sphere. The k^3-dependent term is a *radiative reaction correction*, which applies to any oscillating dipole, be it an elementary molecular dipole or the dipole induced on a small (nano)particle, and follows from the *Abraham–Lorentz equation* [see, e.g., Section 16.2 and Eqs. (16.8) and (16.9) of [20]].

Surprisingly enough, the above Meier and Wokaun [3] recipe in determining $\mathbf{E}_d$ has not yet been carried out analytically for spheroidal particles, which are a special class of ellipsoidal particles having two axes of equal length. Instead, the relevant integrals for a number of spheroid aspect ratios were performed merely numerically (see Subsection 3.A of [5]). Apart from that, literature only knows of two indirect analytic extensions to the case of spheroidal particles. The first derives from the fact that Eq. (4) can be recast as

$$\alpha_{MW} = \frac{V}{4\pi}\frac{\varepsilon - 1}{1 + L_{\text{eff}}(\varepsilon - 1)}, \tag{5}$$

where

$$L_{\text{eff}} = L - \frac{1}{3}x^2 - i\frac{2}{9}x^3, \tag{6}$$

with L being the well-known *geometrical factor* that accounts for the shape of a particle [cf. Eq. (5.32) of [4]; see also Subsection 2.A below]. It was postulated that the spheroid polarizability is obtained by simply replacing the sphere radius a in the size parameter by $(3V/4\pi)^{1/3}$, resulting in

$$L_{\text{eff}} = L - \frac{k^2}{3}\left(\frac{3V}{4\pi}\right)^{2/3} - i\frac{k^3V}{6\pi}, \tag{7}$$

to be substituted in Eq. (5) [6,7]. The point of departure for the second extension was an observation that Eq. (4) can be recast as

$$\alpha_{MW} = \frac{\alpha_R}{1 - \dfrac{k^2}{a}\alpha_R - i\dfrac{2k^3}{3}\alpha_R}, \tag{8}$$

where α_R is the static Rayleigh polarizability of a sphere,

$$\alpha_R = \frac{\varepsilon - 1}{\varepsilon + 2}a^3. \tag{9}$$

Consequently, in the case of a *spheroid* and an applied electric field oriented along a spheroid axis, it was postulated that formally formula (8) still applies, but (i) with α_R replaced by the static spheroid polarizability,

$$\alpha_R = \frac{V}{4\pi}\frac{\varepsilon - 1}{1 + L(\varepsilon - 1)}, \tag{10}$$

($L\equiv 1/3$ for a sphere), and (ii) with the sphere radius a replaced by the spheroid axis half-length l_E, along which the electric field is applied [8–11]. The validity of such an approximation, which was termed a *modified long-wavelength approximation* (MLWA) [8–11], has been partially justified [8] by comparing it to a so-called third approximation of electromagnetic scattering by an ellipsoid in powers of k (i.e., up to the order of k^4) by Stevenson [21]. Despite an obvious difference between α_{MW} and the exact polarizability obtained from Mie's solution for a sphere in the long-wavelength limit (Appendix A),

$$\alpha_{\text{Mie}} = -i\frac{3}{2k^3}T_{E1} = \frac{\varepsilon - 1}{\varepsilon + 2 - (6\varepsilon - 12)\dfrac{x^2}{10} - i\dfrac{2x^3}{3}(\varepsilon - 1)}a^3, \tag{11}$$

which results in a shifted SPR position (Appendix B). The Meier and Wokaun [3] approximation and the resulting MLWA were shown to generate rather reliable results for small metal particles in various studies involving scattering and the local field, SERS, and hyper-Raman enhancements [8–11]. It is worth reminding one here that the static sphere polarizability [Eq. (9)], which is the Rayleigh ($x\to 0$) limit of expression (11), is not unitary (Appendix C) and is insufficient in describing essential features of small metal nanoparticles, such as the size-dependence of a redshift of the SPR (Section 12.1.1. of [4]) and of local field enhancements [3].

In what follows, we show, in spite of claims to the contrary [8], that a direct extension of the Meier and Wokaun prescription [3] to spheroidal particles is possible and obtain the spheroid polarizability

$$\alpha_{MW} = \frac{\alpha_R}{1 - \dfrac{k^2}{l_E}D\alpha_R - i\dfrac{2k^3}{3}\alpha_R}, \tag{12}$$

where α_R is given by Eq. (10) and D is a *dynamic geometrical factor* ($D\equiv 1$ and $l_E=a$ for a sphere). The outline of the paper is as follows. In Section 2, the parallel, $dE_{d,\parallel}$, and perpendicular, $dE_{d,\perp}$, components of the depolarization field are introduced. In Subsection 2.A the volume integral of a static ($\sim 1/r^3$ term) component of $d\mathbf{E}_d$ is per-

formed for a particle of any general shape. In Subsection 2.B explicit formulas for the dynamic geometrical factors in terms of the standard geometrical factors of electrostatics are provided. In Subsection 2.C the resulting $\mathbf{E}_d$ is determined and it is shown that the heuristic Meier and Wokaun [3] recipe in determining $\mathbf{E}_d$ is equivalent to a long-wavelength limit up to the order of k^3 of the Green's function technique. The results and their applicability are discussed in Section 3. Subsection 3.A shows that the resulting Meier and Wokaun [3] long-wavelength approximation (MWLWA) exhibits a redshift compared to exact T-matrix results. Subsection 3.B shows that, at least for a sphere, it is possible to get rid of the redshift by assuming a weak nonuniformity of the fields $\mathbf{E}_{int}$ and $\mathbf{P}$ inside a particle, which can be fully accounted for by a renormalization of the dynamic geometrical factors. We then conclude with Section 4.

2. DEPOLARIZATION FIELD

The first two steps of the Meier and Wokaun [3] prescription for calculating $\mathbf{E}_d$ can be performed rather straightforwardly. Radial and tangential fields produced by a retarded dipole $[p]=pe^{ikr}$ are (Section 2.2.3 of [22])

$$E_r = 2\cos\theta\left(\frac{[p]}{r^3}+\frac{[\dot{p}]}{cr^2}\right),$$

$$E_\theta = \sin\theta\left(\frac{[p]}{r^3}+\frac{[\dot{p}]}{cr^2}+\frac{[\ddot{p}]}{c^2r}\right). \tag{13}$$

On assuming a harmonic time dependence,

$$[\dot{p}] = -i\omega[p], \quad [\ddot{p}] = -\omega^2[p], \tag{14}$$

expanding e^{ikr} in powers of kr, retaining terms up to order k^3, and using

$$E_\parallel = E_r\cos\theta - E_\theta\sin\theta,$$

$$E_\perp = E_r\sin\theta + E_\theta\cos\theta,$$

one obtains in the spherical coordinates tight up with the elementary dipole element $d\mathbf{p}$, and with the polar coordinate aligned along the direction of the polarization vector,

$$dE_{d,\parallel} = \left[\frac{1}{r^3}(3\cos^2\theta-1)+\frac{k^2}{2r}(\cos^2\theta+1)+i\frac{2}{3}k^3\right]P\mathrm{d}V, \tag{15}$$

$$dE_{d,\perp} = \left[\frac{3\sin\theta\cos\theta}{r^3}+\frac{k^2\sin\theta\cos\theta}{2r}\right]P\mathrm{d}V. \tag{16}$$

In addition to [3], the formula for $dE_{d,\perp}$ has also been provided, since, *a priori*, it is not clear that the perpendicular component vanishes for particles of a general shape. To simplify the notation, we have set $\varepsilon_h=1$ herein above and below.

Note in passing that $dE_{d,\perp}$ does not have a radiating (proportional to k^3) component. On assuming $\mathbf{E}_{int}$, and hence also $\mathbf{P}$, being *homogeneous* inside a particle (by virtue of the *weak Eshelby conjecture* [18] this is always satisfied for a spheroid, and in particular for $\mathbf{E}_0$ oriented along a spheroid principal axis), one finds in the spherical coordinates tight up with a particle center

$$d\mathbf{E}_d = \left\{\frac{3\hat{\mathbf{r}}(\mathbf{P}\cdot\hat{\mathbf{r}})-\mathbf{P}}{r^3}+\frac{\hat{\mathbf{r}}(\mathbf{P}\cdot\hat{\mathbf{r}})+\mathbf{P}}{2r}k^2+i\frac{2k^3}{3}\mathbf{P}\right\}\mathrm{d}V, \tag{17}$$

where $\hat{\mathbf{r}}=\mathbf{r}/r$ is a unit vector. To this end, it remains to perform the final step of integrating $\mathbf{E}_d$ over the particle volume. The k^3 term in Eq. (17) integrates straightforwardly to $i(2k^3V\mathbf{P})/3$. However, the volume integrals of the remaining static ($\sim 1/r^3$) and dynamic ($\sim k^2$) components of $d\mathbf{E}_d$ in Eq. (17) amount to calculating the potentials in a source region (cf. Section VI.2. of [23]) and are the most demanding steps of the Meier and Wokaun [3] prescription.

A. Static Depolarization

In this section it will be demonstrated that the volume integral of the static term can be performed for a particle of any general shape. First note that the $1/r^3$ term of the depolarization field $d\mathbf{E}_d$ in Eq. (17) corresponds to a *static* dipole field [cf. Eq. (4.13) of Section 4.1 of Jackson's book [20]]. Therefore, upon integrating the static component $d\mathbf{E}_{d;1/r^3}$ of $d\mathbf{E}_d$ over a particle volume one expects to arrive at the electrostatics result [19]

$$\mathbf{E}_{d;1/r^3} = -4\pi\bar{\mathbf{L}}\cdot\mathbf{P}, \tag{18}$$

where the symmetric (Section 5A of [24]) tensor

$$\bar{\mathbf{L}} = \frac{1}{4\pi}\oint_{\partial V}\frac{\mathrm{d}\mathbf{S}\otimes\hat{\mathbf{r}}}{r^2} = \oint_{\partial V}\frac{\hat{\mathbf{r}}\otimes\mathrm{d}\mathbf{S}}{r^2}, \tag{19}$$

with $\otimes$ denoting the tensor product of vectors (dyadic) in $\mathbb{R}^3$, is defined by the surface integral over the surface ∂V of V [cf. Eqs. (18b) and (44b) of [24]]. $\bar{\mathbf{L}}$ can be concisely interpreted as a *generalized depolarizing dyadic* of a particle (Section 5C of [24]). In particular, for a spheroid $\bar{\mathbf{L}}$ is a diagonal tensor, $\bar{\mathbf{L}}=\mathrm{diag}(L_x,L_y,L_z)$, with L_j being the familiar spheroid *geometrical factors* of electrostatics. Assuming the spheroid z axis be the rotational axis, one finds [4,19]

$$L_z = \begin{cases}\dfrac{1-e^2}{e^3}(-e+\operatorname{arctanh} e) & \text{prolate}\\[2ex] \dfrac{1}{e^2}\left(1-\dfrac{\sqrt{1-e^2}}{e}\arcsin e\right) & \text{oblate}\end{cases}, \tag{20}$$

where the hyperbolic arctan can be expressed as

$$\operatorname{arctanh} e = \frac{1}{2}\ln\frac{1+e}{1-e}, \tag{21}$$

and the *eccentricity*

$$e^2 = \begin{cases} \dfrac{c^2 - a^2}{c^2} & \text{prolate} \\ \dfrac{a^2 - c^2}{a^2} & \text{oblate} \end{cases}. \tag{22}$$

The remaining static geometrical factors $L_x = L_y$ can be determined by using the sum rule (see p. 146, [4])

$$L_x + L_y + L_z = 1. \tag{23}$$

Our definition of the eccentricity, which has been defined as the ratio of the difference of the squares of the major and minor semiaxes divided by the square of the major semiaxis, is identical to that of Bohren and Huffman [cf. Eq. (5.33) of [4]; for an oblate spheroid, Landau and Lifshitz [19] employed a different definition of e]. The shape of the oblate spheroid then ranges from a disk ($e=1$) to a sphere ($e=0$); that of the prolate spheroid ranges from a needle ($e=1$) to a sphere ($e=0$).

To this end, note that

$$d\mathbf{E}_{d;1/r^3} = \frac{3\hat{\mathbf{r}}(\mathbf{P}\cdot\hat{\mathbf{r}}) - \mathbf{P}}{r^3} dV = [\bar{\mathbf{G}}_0(\mathbf{r})\cdot\mathbf{P}]\mathrm{d}V, \tag{24}$$

where

$$\bar{\mathbf{G}}_0(\mathbf{r}) = \boldsymbol{\nabla}\otimes\boldsymbol{\nabla}\left(\frac{1}{r}\right) = \frac{3\hat{\mathbf{r}}\otimes\hat{\mathbf{r}} - \mathbf{1}}{r^3}, \tag{25}$$

with $\mathbf{1}$ being a unit tensor, is a free space Green's function in electrostatics. Thus the integral over a particle volume formally reduces to

$$\mathbf{E}_{d;1/r^3} = \int_V [\bar{\mathbf{G}}_0(\mathbf{r})\cdot\mathbf{P}]\mathrm{d}V. \tag{26}$$

However, a severe obstacle in performing the integral over a particle volume and at arriving at the final result [Eq. (18)] is a nonintegrable $1/r^3$ singularity of the integrand, which is now hidden in $\bar{\mathbf{G}}_0(\mathbf{r})$. Indeed, such a $1/r^3$ singularity violates the sufficient condition of convergence of the Kellogg lemma (Appendix D) and the integral in Eq. (26) does not converge. The $1/r^3$ singularity renders the integrals, such as that in Eq. (26), *ambiguous* and depending on the way the integration is performed in close proximity to the singularity [24]. For instance, following the convention suggested in Jackson's textbook (see the discussion following Eq. (4.20) of Section 4.1 of [20]), the volume integral for a sphere would yield zero, leading to an obviously wrong result. Apparently, this has been the chief reason why the attempts to prove the general formula (18) within the Meier and Wokaun [3] framework have foundered.

Such nonintegrable $1/r^3$ singularities are at the very heart of the applicability of the Green's function method in the source regions in electrodynamics and electrostatics. According to Section 5C of [24], if it is demanded that $\mathbf{E}_{d;1/r^3}$ on the left-hand side (lhs) of Eq. (26) corresponds to the electric field inside the source region generated by a given distribution of $\mathbf{P}$, the integral in Eq. (26) has to be interpreted as

$$\mathbf{E}_{d;1/r^3} = \lim_{\delta\to 0}\int_{V-V_\delta} [\bar{\mathbf{G}}_0(\mathbf{r})\cdot\mathbf{P}]\mathrm{d}V - 4\pi\bar{\mathbf{L}}\cdot\mathbf{P}, \tag{27}$$

which is Eq. (53a) of [24] rewritten in Gauss units. Here V_δ is an arbitrary small volume surrounding the singularity, called the *principal* volume, and the depolarization tensor $\bar{\mathbf{L}}$ is that defined by Eq. (19), but with ∂V replaced by ∂V_δ. Although each of the two terms on the right-hand side (rhs) of Eq. (27) is dependent on the shape of V_δ, the rhs of Eq. (27) is not [24]. Now, by expanding over the teaching of [24], we follow a point of crucial importance. The infinitesimally small principal volume V_δ is not necessary in Eq. (27), provided that (i) one has advance knowledge that $\mathbf{P}$ is *uniform* over the particle volume, and (ii) V_δ is of the same shape as V. By the latter it is meant that V_δ is nothing but a scaled down version of V under the scaling $\mathbf{r}\to C\mathbf{r}$, with C being a real constant. Under the above two hypotheses then, on recalling Eq. (25),

$$\int_{V-V_\delta} [\bar{\mathbf{G}}_0(\mathbf{r})\cdot\mathbf{P}]\mathrm{d}V = \boldsymbol{\nabla}\int_{V-V_\delta} \boldsymbol{\nabla}\cdot\left(\frac{\mathbf{P}}{r}\right)\mathrm{d}V = \boldsymbol{\nabla}\oint_{\partial(V-V_\delta)}\left(\frac{\mathbf{P}\cdot\mathrm{d}\mathbf{S}}{r}\right) \equiv 0, \tag{28}$$

because the surface integration over the respective scaled surfaces V_δ and V cancels in the sum. First, the respective surface integrals have a scale invariant integrand. Second, consider the respective outward surface normals of the volume $V-V_\delta$ at the points of the intersection of a ray emanating from the origin with the surfaces of V_δ and V as illustrated in Fig. 1. Obviously, an outward surface normal on the surface of ∂V_δ of the volume $V-V_\delta$ corresponds to the inward pointing normal of the volume V_δ. Therefore, the normals at the points, which are related by the scaling, necessarily point in the opposite directions. At the same time one makes use of the property that the defining integral [Eq. (19)] for $\bar{\mathbf{L}}$ is invariant under the scaling $\mathbf{r}\to C\mathbf{r}$ of V_δ and only depends on the shape of V_δ. Thus,

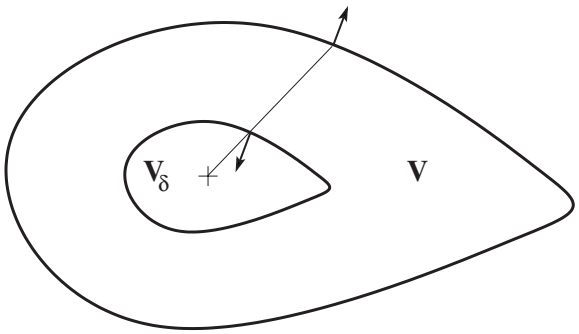

Fig. 1. Illustration of the integration [Eq. (28)] over the surface of the volume $V-V_\delta$. The surface normals at the intersection of each ray emanating from the origin with the surfaces of V_δ and V, which are related by scaling, necessarily point in opposite directions.

$$\mathbf{E}_{d;1/r^3} = -4\pi\bar{\mathbf{L}}\cdot\mathbf{P}, \tag{29}$$

irrespective if V_δ or scaled-up V is employed in the defining integral [Eq. (19)] for $\bar{\mathbf{L}}$, thereby yielding the expected result [Eq. (18)].

In an alternative derivation one can get rid of the principal volume considerations by realizing that $d\mathbf{E}_{d;1/r^3}$ can be recast as

$$d\mathbf{E}_{d;1/r^3} = \frac{3\hat{\mathbf{r}}(\mathbf{P}\cdot\hat{\mathbf{r}})-\mathbf{P}}{r^3}\mathrm{d}V = -\,\mathrm{d}V\,\boldsymbol{\nabla}\left(\frac{\mathbf{P}\cdot\mathbf{r}}{r^3}\right). \tag{30}$$

This enables one to determine $\mathbf{E}_{d;1/r^3}$ as

$$\mathbf{E}_{d;1/r^3} = -\boldsymbol{\nabla}\Phi = -\boldsymbol{\nabla}\int_V \frac{\mathbf{P}\cdot\mathbf{r}}{r^3}\mathrm{d}V, \tag{31}$$

where the potential Φ possesses an integrable $1/r^2$ singularity (Appendix D). Since $\mathbf{r}/r^3 = -\boldsymbol{\nabla}(1/r)$, the integral in Eq. (31) can be, on using the Gauss theorem, recast into the integral over the surface ∂V of V resulting in

$$\mathbf{E}_{d;1/r^3} = \boldsymbol{\nabla}\oint_{\partial V}\frac{\mathrm{d}\mathbf{S}\cdot\mathbf{P}}{r}, \tag{32}$$

where the surface element $\mathrm{d}\mathbf{S}$ points along the outward normal to the surface ∂V of V. It is now permitted to take $\boldsymbol{\nabla}$ behind the integration sign. The result can be shown to be equivalent to

$$\mathbf{E}_{d;1/r^3} = -\left(\oint_{\partial V}\frac{\hat{\mathbf{r}}\otimes\mathrm{d}\mathbf{S}}{r^2}\right)\cdot\mathbf{P} = -4\pi\bar{\mathbf{L}}\cdot\mathbf{P}, \tag{33}$$

which is the expected result of Eq. (18).

The above two derivations of the general formula [Eq. (18)] are an example that a simple interchange of the operations of differentiation and integration, such as taking $\boldsymbol{\nabla}$ behind the integration sign in Eq. (30), is in general forbidden when an integrand with a nonintegrable $1/r^3$ or a higher-order singularity results [24]. If a $1/r^3$ singularity arises, it is necessary to apply the limiting procedure with a "principal volume" V_δ excluding the singularity, as exemplified by Eq. (27) [24].

B. Dynamic Depolarization

In the present section, the integral of the dynamic term for a spheroidal particle will be performed. In contrast to a nonintegrable $1/r^3$ singularity, a $1/r$ singularity is an integrable one (Appendix D). Therefore, one can consider the volume integrals of the respective $1/r$ terms of $dE_{d,\parallel}$ and $dE_{d,\perp}$ given by Eqs. (15) and (16), separately. Consider an electric field applied along any of the principal axes of a spheroid. A spheroid is invariant under the rotation by an angle π around its principal axes. Hence, any of the spheroid principal axes is simultaneously the axis of at least discrete twofold rotational symmetry, or of discrete rotational symmetry C_2 of the second order. But any depolarization element $dE_{d,\perp}$ changes its orientation to the opposite one under the rotation by an angle π around the spheroid axis aligned with the electric field. Therefore,

$$\int_V \mathrm{d}E_{d,\perp;1/r} \equiv 0, \tag{34}$$

where $dE_{d,\perp;1/r}$ stands for the $1/r$ terms in Eq. (16). Obviously, the latter conclusion applies to any particle enjoying a C_2 axis of symmetry and with an electric field being applied along the axis.

In what follows, the z axis will always be the rotational axis of a spheroid with the half-length c and with perpendicular axes $a=b$. Turning now to the $1/r$ terms of $dE_{d,\parallel;1/r}$, it will be demonstrated here that, for the electric field applied along the rotational axis of a spheroid,

$$\int_V \mathrm{d}E_{d,\parallel;1/r} = k^2\int_V \frac{\cos^2\theta+1}{2r}\mathrm{d}V = \frac{k^2V}{l_E}D_z, \tag{35}$$

where $l_E=c$ and the *dynamic geometrical factor* D_z can be expressed in terms of the *static geometrical factors* as follows:

$$D_z = \frac{3}{4}\times\begin{cases}\dfrac{1+e^2}{1-e^2}L_z+1 & \text{prolate}\\ (1-2e^2)L_z+1 & \text{oblate}\end{cases}. \tag{36}$$

In what follows, we denote the dynamic geometrical factors for an electric field applied parallel and perpendicular to the rotational axis of a spheroid temporarily as $D_\parallel$ and $D_\perp$, respectively. For a uniform electric field applied along the direction perpendicular to the rotational axis of a spheroid, $l_E=a=b$, the respective dynamic geometrical factors $D_\perp=D_x=D_y$ can be determined from the knowledge of D_z and of the following sum rule:

$$2\frac{c}{a}D_\perp + D_z = 3\times\begin{cases}\dfrac{1}{e}\operatorname{arctanh} e & \text{prolate}\\ \dfrac{\sqrt{1-e^2}}{e}\arcsin e & \text{oblate}\end{cases}. \tag{37}$$

The behavior of the dynamic geometrical factors is shown in Fig. 2. For $e\to 0$ all the factors approach the value of 1, irrespective of whether the spheroid is prolate or oblate. The latter ensures that Eq. (12) goes smoothly to Eq. (8) in the limit. This limiting behavior can also be established on using the asymptotic formulas in [25], which yield

$$D_\parallel = D_z \sim \begin{cases}1-2e^2/5 & \text{prolate}\\ 1+2e^2/5 & \text{oblate}\end{cases}, \tag{38}$$

$$D_\parallel + 2\frac{c}{a}D_\perp \sim 3\times\begin{cases}1+e^2/3+e^4/5+\mathcal{O}(z^6) & \text{prolate}\\ 1-e^2/3-2e^4/15+\mathcal{O}(e^6) & \text{oblate}\end{cases}. \tag{39}$$

On recalling the definition [Eq. (21)] of the hyperbolic arctan, the factor $D_\parallel$ of a prolate spheroid can be shown to diverge logarithmically as $\sim -(3/4)\ln(1-e)$ for $e\to 1$. On combining this limiting behavior with Eq. (37), $D_\perp \propto -\sqrt{1-e}[\ln(1-e)]\to 0$ as $e\to 1$. For oblate spheroids, one finds on using $\arcsin 1=\pi/2$ and the fifth equation in [25], that $D_\parallel \sim 3\pi c/(8a)\to 0$ as $e\to 1$. On combining this limiting behavior with Eq. (37), one finds that

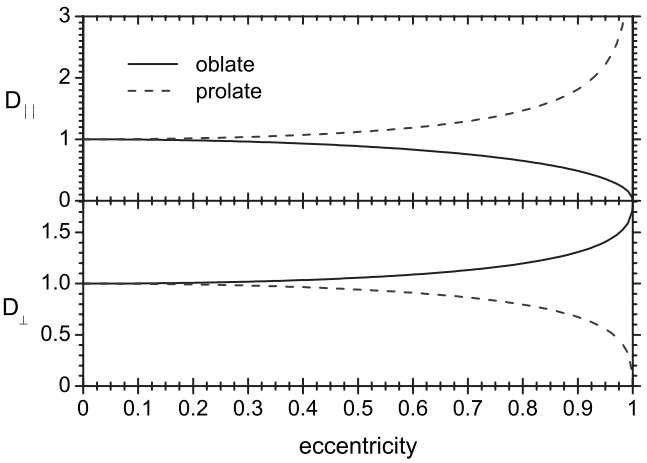

Fig. 2. Dynamic geometrical factors $D_\parallel$ and $D_\perp$ for an electric field applied parallel and perpendicular to the spheroid rotational axis, respectively. As an illustration, for spheroids with the aspect ratio 2:1, 3:1, 4:1, 5:1, and 6:1 the eccentricity takes on the values of $\approx$0.866, $\approx$0.943, $\approx$0.968, $\approx$0.98, and $\approx$0.986, respectively. For prolate spheroids, $D_\parallel \to \infty$, whereas for oblate spheroids $D_\perp = 9\pi/16$ as $e \to 1$.

$D_\perp = (9\pi)/16 \approx 1.767$ as $e \to 1$. This is confirmed by Fig. 2, which displays the behavior of $D_\perp$ and $D_\parallel$.

Summary of the proof. An ellipsoid defined by

$$\frac{x^2}{a^2} + \frac{y^2}{b^2} + \frac{z^2}{c^2} = 1, \tag{40}$$

is, upon the substitution

$$x = ax', \quad y = by', \quad z = cz', \tag{41}$$

transformed into a unit sphere,

$$(x')^2 + (y')^2 + (z')^2 = 1. \tag{42}$$

The radius vector square is

$$r^2 = a^2(x')^2 + b^2(y')^2 + c^2(z')^2, \tag{43}$$

and the corresponding primed and unprimed volume elements are related by $dV = abc\,dV'$. On using cylindrical coordinates (ρ, z', φ),

$$r^2 = a^2\rho^2 + c^2(z')^2 = a^2[\rho^2 + (c^2/a^2)(z')^2],$$

$$dV = a^2 c\rho d\rho dz' d\varphi. \tag{44}$$

For an electric field applied along the jth spheroid principal axis

$$\cos^2\theta + 1 = \frac{1}{r^2}(x_j^2 + r^2), \tag{45}$$

where $(x_1, x_2, x_3) = (x, y, z)$. Thus, for a field applied along the z axis, one has to deal with the integral

$$\int_V \frac{\cos^2\theta + 1}{2r} dV = 2\pi ac \int_0^1 dz' \int_0^{\sqrt{1-(z')^2}} \frac{\rho^2 + 2(c^2/a^2)(z')^2}{[\rho^2 + (c^2/a^2)(z')^2]^{3/2}} \rho d\rho, \tag{46}$$

where the trivial integration over φ has already been performed and use was made of the mirror symmetry $z' \to -z'$ of the integrand. In the case of the sum $(c/a) \times (D_x + D_y) + D_z$, the result is proportional to $\int_V (dV/2r)$, which is determined in Appendix E. The initial integration over the polar coordinate $\rho \in [0, \sqrt{1-(z')^2}]$ is identical for both prolate and oblate spheroids and can be straightforwardly performed on using the quadrature formulas in [25]. A subsequent integration over the coordinate $z' \in (0,1)$ then depends on a particular spheroid type. In the case of D_z, the latter can be performed on using the respective quadrature formulas in [25].

C. Final Result for a Uniform $\mathbf{E}_{int}$

On combining the partial results, Eqs. (18) and (35), together with the radiation reaction term, one arrives for a spheroidal particle at the depolarization field

$$\mathbf{E}_d = -4\pi\left(\bar{\mathbf{L}} - \frac{k^2 V}{4\pi}\bar{\mathbf{D}} - i\frac{2k^3}{3}\frac{V}{4\pi}\mathbf{1}\right)\cdot\mathbf{P}, \tag{47}$$

where, like the static geometrical factors, the dynamic geometrical factors have been assembled into a diagonal dynamic depolarization tensor $\bar{\mathbf{D}} = \mathrm{diag}(D_x/a, D_y/b, D_z/c)$. After substituting the result for $\mathbf{E}_d$ back into the defining equation (3) for the polarization $\mathbf{P}$ aligned along the spheroid principal axis, the polarizability [Eq. (12)] results. Thereby, in contrast to Stevenson's approximation [21], the Meier and Wokaun [3] prescription enables one to capture the essential size-dependence features of the polarizability of small spherical and spheroidal particles [cf. Eqs. (4) and (12)] in a single compact analytical formula. However, a complete description of the size dependence of the polarizability requires that the size dependence of the dielectric function is also taken into account [7–11] (for recent progress see [26]).

Finally, we show that, not unexpectedly, the Meier and Wokaun [3] recipe in determining $\mathbf{E}_d$ is equivalent to the long-wavelength limit up to the order of k^3 of the exact formula of the Green's function technique

$$\mathbf{E}_d = k^2 \lim_{\delta\to 0} \int_{V-V_\delta} [\bar{\mathbf{G}}(\mathbf{r})\cdot\mathbf{P}]dV - 4\pi\bar{\mathbf{L}}\cdot\mathbf{P} \tag{48}$$

(the formula, Eq. (48), follows on substituting $\mathbf{J} = -i4\pi\omega\varepsilon_h\mathbf{P}$ in Eq. (18a) of [24]), where

$$\bar{\mathbf{G}}(\mathbf{r},\mathbf{r}') = \bar{\mathbf{G}}(\mathbf{R}) = \left(\mathbf{1} + \frac{\nabla\otimes\nabla}{k^2}\right)\frac{e^{ikR}}{R}, \tag{49}$$

with $\mathbf{R} = \mathbf{r} - \mathbf{r}'$ and $R = |\mathbf{R}|$, is the so-called *electric Green's function* for an infinite homogeneous medium. Indeed, on substituting the long-wavelength expansion of $\bar{\mathbf{G}}$ in powers of k,

$$\bar{\mathbf{G}}(\mathbf{r}) = \frac{1}{k^2}\left[\frac{3\hat{\mathbf{r}}\otimes\hat{\mathbf{r}}-1}{r^3} + \frac{\hat{\mathbf{r}}\otimes\hat{\mathbf{r}}+\mathbf{1}}{2r}k^2 + i\frac{2k^3}{3}\right] + \mathcal{O}(k^2), \tag{50}$$

into Eq. (48) one finds that the resulting integrand is nothing but the expression in curly brackets in Eq. (17).

3. DISCUSSION AND OUTLOOK

A. Numerical Results

In Fig. 3, the results for the extinction efficiency (extinction cross section divided by πr_{ev}^2, where r_{ev} is an equivalent-volume-sphere radius) of an oblate silver spheroid with r_{ev} of 20 nm are shown for the major to minor axis ratio of 5:1. Figure 4 shows the same for a prolate silver spheroid with an equivalent-volume-sphere radius r_{ev} of 40 nm and the major to minor axis ratio of 4:1. In the case of various long-wavelength approximations (LWA), extinction cross sections were calculated according to Eq. (C3) with $2ik^3\alpha/3$, where α is an appropriate polarizability, being substituted for T_{E1}. The exact T-matrix results (solid curve) include the contribution of higher-order multipoles and have been obtained by the Mishchenko code [14] with a recent improvement [15]. The T-matrix code, freely available at http://www.wave-scattering.com/codes.html, was run for a plane wave incidence perpendicular to the rotational symmetry axis (i.e., with the code parameters THET0=THET=90 and PHI0=PHI=0). All the plots were generated on using the bulk silver dielectric function [27] without any size correction.

In agreement with the analytic result for spherical particles (Appendix B), the resulting MWLWA [Eq. (12); dashed-dotted lines] is found to be *redshifted* with regard to the exact T-matrix results. Overall, MWLWA appears to provide only a minor improvement over the conventional MLWA [Eq. (8); dotted curve], which is characterized by constant dynamic geometrical factors

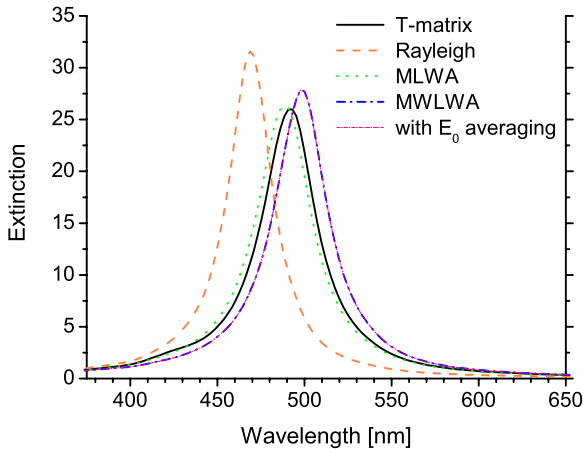

Fig. 3. (Color online) Comparison of the extinction efficiency obtained in the Rayleigh limit, by MLWA, and MWLWA, against the exact T-matrix method results. The results are shown for an oblate silver spheroidal particle with the major to minor axis ratio of 5:1 and an equivalent-volume-sphere radius of 20 nm ($a=b\approx 34.2$ and $c\approx 6.84$ nm). Electric field is oriented perpendicular to the rotational symmetry axis.

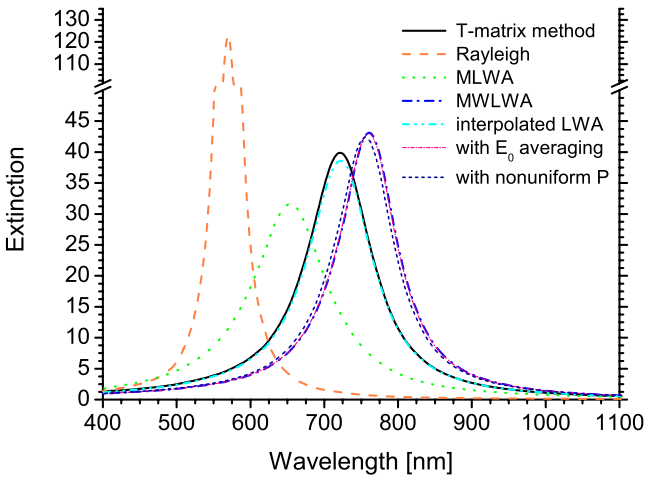

Fig. 4. (Color online) Comparison of the extinction efficiency obtained in the Rayleigh limit, by MLWA, MWLWA, interpolated LWA, and MWLWA with a nonuniform P against the exact T-matrix method results. The results are shown for a prolate silver spheroidal particle with the major to minor axis ratio of 4:1 and an equivalent-volume-sphere radius of 40 nm ($a=b\approx 25.2$ nm and $c\approx 100.8$ nm). Electric field is oriented along the rotational symmetry axis.

$$\tilde{D}_{\parallel} = \tilde{D}_{\perp} = 1. \tag{51}$$

MWLWA yields better results for prolate spheroids, but it is worse for oblate spheroids. Clearly, the Rayleigh approximation [Eq. (10); dashed curves] is not suited for the spheroidal particle considered.

B. Renormalized Dynamic Geometrical Factors

So far, the field $\mathbf{E}_{int}$, and the resulting polarization $\mathbf{P}$, within a particle have been assumed to be homogeneous. Yet, for the particle dimensions considered here, variations of $\mathbf{E}_{int}$ in excess of 10% are not unusual. Moreover, MWLWA singles the particle center out as a special point. However, at least for a sphere, $|\mathbf{E}_{int}|$ takes on a local minimum at the particle center for wavelengths around the SPR position. Therefore, calculating $\mathbf{E}_d$ at a particle center may not provide the best approximation to an average $\mathbf{E}_d$ inside the particle.

Obviously, the only way to improve MWLWA is to take into account an actual field profile inside a particle. In fact, in the case of a sphere, a nonuniform field profile inside a particle can account for the whole redshift. Indeed, according to Stevenson [21], the leading correction to a uniform $\mathbf{E}_{int}$ for spheroidal particles is of the order of k^2. By virtue of Eqs. (15) and (17), it is enough to consider only the singular $1/r^3$ term, since corrections to the remaining k^2 and k^3 terms will produce corrections of the order of at least k^4. A point of crucial importance is that the angular integration of the $1/r^3$ term yields identically zero. Therefore, only the θ-dependent part of the full correction, which would modify the angular part of the $1/r^3$ term so that it yields a nonzero contribution, is needed for our purposes. Assuming $\mathbf{E}_0$ polarized along the axis of rotational symmetry, let us consider a simple angular dependence of the polarization of the form

$$\mathbf{P}_c = \mathbf{P}\left(1 + \frac{1}{2}k^2 r^2 \sin^2\theta\right), \tag{52}$$

which satisfies all the above requirements including a local minimum of $|\mathbf{P}|$ at the particle center. On substituting such a weakly nonuniform $\mathbf{P}$ back into Eqs. (15) and (17), the net effect is to replace the dynamic depolarization term in Eqs. (15) and (17) by

$$k^2 \frac{5\cos^2\theta - 3\cos^4\theta}{2r} P = \frac{5\hat{r}^2 - 3}{2r}\hat{\mathbf{r}}(\mathbf{P}\cdot\hat{\mathbf{r}})k^2. \tag{53}$$

For a sphere, one arrives on using Eq. (88) at

$$\mathbf{E}_d = -\frac{4\pi}{3\varepsilon_h}\left(1 - \frac{4}{5}x^2 - i\frac{2}{3}x^3\right)\mathbf{P}, \tag{54}$$

being substituted for Eq. (2). It can be straightforwardly verified that this delivers the polarizability, which yields the SPR peak position in the extinction efficiency coinciding with the exact result [Eq. (B1)] by Bohren and Huffman [4] (cf. Appendix B).

In the spheroid case, the very same angular dependence of polarization of Eq. (52) leads to the dynamic geometrical factors D_z of Eq. (55) being substituted by (see quadrature formulas of Appendix E)

$$D_{z;rn} = \frac{3}{4} \times \begin{cases} \dfrac{(5e^2-3)}{(1-e^2)e^2}L_z + \dfrac{1}{e^2} & \text{prolate} \\ \dfrac{1-e^2}{e^2}[(2e^2+3)L_z - 1] & \text{oblate} \end{cases}. \tag{55}$$

Clearly, the dependence of Eq. (52) does not account for the whole redshift in the spheroid case (short-dashed curve in Fig. 4). An argument that some other spatial dependence of the polarization followed by a subsequent renormalization of the dynamic geometrical factors may get rid of the whole redshift in the spheroid case is provided by the following empirical dynamic geometric factor:

$$D_{av} = 0.37 + 0.63D. \tag{56}$$

The results generated by the interpolated LWA (dashed-dotted-dotted curve), which makes use of the factors, are shown in Figs. 4 and 5. In all the cases, electric field is oriented along the rotational symmetry axis. The interpolated LWA accurately matches the SPR position, height, and linewidth of the exact results for noble particles with an equivalent-volume-sphere radius of up to ≈50 nm in the visible. (A discussion of this criterion for spherical particles, which derives from the estimate of relative magnitudes of the electric dipole moment on one hand against that of the magnetic dipole moment and electric quadrupole moment on the other hand, can be found on p. 583 of [3] and in the very last two paragraphs of Subsection 3.B of [5].) Note in passing that the linewidth Γ directly determines the plasmon dephasing time $T_2 = 2\hbar/\Gamma$, where $\hbar$ is the Planck constant, the quality factor Q of the resonance at the SPR frequency ω_{res} via the formula $Q = \omega_{res}/\Gamma$, and the local field enhancement factor $|f|$ (in a harmonic model $|f| = Q$).

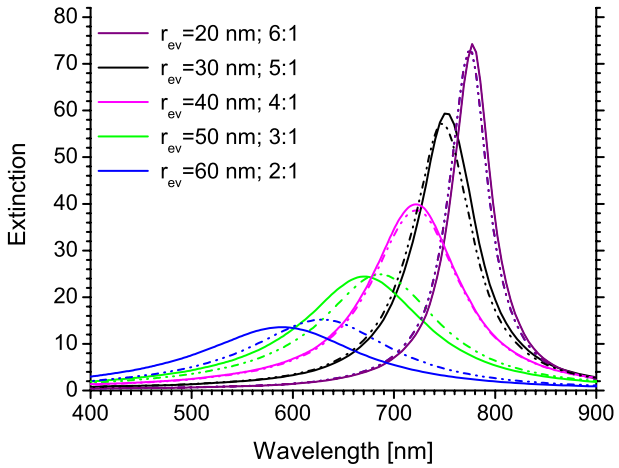

Fig. 5. (Color online) Comparison of the interpolated LWA (dashed-dotted-dotted curves) against the exact T-matrix method results (solid curves) for prolate silver spheroidal particles. From left to right, spheroids with the major to minor axis ratios increasing from 2:1 to 6:1 and with $(r_{ev};a=b;c) \approx (60;47.6;95.2)$, (50; 34.7; 104), (40; 25.2; 100.8), (30; 17.5; 87.7), and (20;11;66) nm. Electric field is oriented along the rotational symmetry axis.

C. Related Approaches

In an attempt to improve the MWLWA, Meier and Wokaun [3] and Wokaun [7] have proposed to replace the exciting field $\mathbf{E}_0$ with its volume average. In the case of a plane wave incident on a sphere this results, up to the order of x^2, in the exciting field

$$\frac{1}{V}\int_V \mathbf{E}_0 \cos(\mathbf{k}\cdot\mathbf{r})\mathrm{d}V \approx \mathbf{E}_0\left(1 - \frac{x^2}{10}\right). \tag{57}$$

This in turn leads to $\varepsilon - 1$ in the numerator of Eq. (4) being replaced by $(\varepsilon-1)(1-x^2/10)$ [3,7], or, up to the order of x^3, equivalently to the polarizability

$$\alpha_{MW;m} = \frac{\varepsilon - 1}{\varepsilon + 2 - (9\varepsilon - 12)\dfrac{x^2}{10} - i\dfrac{2x^3}{3}(\varepsilon - 1)}a^3. \tag{58}$$

At first sight, the latter polarizability appears to be closer to the exact expression (11), yet it still leads to the very same offset SPR position [see Eq. (B2)] as its predecessor of Eq. (4) does. The same procedure for a spheroid results in either $(\varepsilon-1)(1-k^2c^2/10)$ or $(\varepsilon-1)(1-k^2a^2/10)$ replacing $\varepsilon - 1$ in the numerator of Eq. (10), depending on whether $\mathbf{k}$ is parallel or perpendicular to the axis of axial symmetry. However, the Meier and Wokaun [3] and Wokaun [7] proposal is different from ours, since it does not lead to any change in dynamic geometric factors. Moreover, as Figs. 3 and 4 demonstrate, replacing the exciting field $\mathbf{E}_0$ with its volume average (short-dashed-dotted curve in figures) does not bring any appreciable change in the calculated results for the extinction efficiency.

Interestingly enough, the work by Kuwata *et al.* [28] has anticipated dynamic depolarization factors by purely empirical formula obtained by best fit to numerical results, in which case dynamic depolarization factors were fitted by a polynomial of the third order in L_z. In contrast, formula (56) together with the analytic results of the pa-

per suggest that a linear L_z dependence, but with "e"-dependent coefficients, may be enough.

4. SUMMARY AND CONCLUSIONS

A compact analytical formula [Eq. (47)] was provided for the depolarization field $\mathbf{E}_d$ of a spheroidal particle by carrying out explicitly the steps of the Meier and Wokaun procedure [3]. For the static component of $\mathbf{E}_d$, the electrostatic formula [Eq. (18)] valid for a particle of a general shape was rederived within the Meier and Wokaun [3] framework. The dynamic depolarization component of $\mathbf{E}_d$ was shown to depend on *dynamic* geometrical factors. Explicit expressions [Eqs. (36) and (37)] for the dynamic geometrical factors were given in terms of the standard geometrical factors [Eqs. (20) and (23)] of electrostatics. Limitations of the Meier and Wokaun [3] procedure, which was shown to be equivalent to a long-wavelength limit of the Green's function technique and to exhibit a redshift compared to exact T-matrix results, were examined. A weak θ-dependent nonuniformity of the polarization $\mathbf{P}$ inside a particle was shown to induce a change in the dynamic geometrical factors [Eqs. (54) and (55)]. On the example of a sphere it was demonstrated that such a change can compensate for the redshift of the Meier and Wokaun [3] long-wavelength approximation (LWA). An appropriate θ-dependent nonuniformity of $\mathbf{P}$, the existence of which has been indirectly vindicated by the empirical interpolated LWA and that is almost an exact match of the exact T-matrix results, may do the same for spheroids. Results of the present paper may be relevant for various plasmonic, or nanoantenna, applications of spheroidal particles with a dominant electric dipole scattering whenever it is necessary to go beyond the Rayleigh approximation and capture the essential size-dependent features of scattering, local fields, SERS, hyper-Raman, and second-harmonic-generation enhancements [8,9], decay rates, and photophysics of dipolar arrays [5].

APPENDIX A: T-MATRIX IN THE LONG-WAVELENGTH LIMIT FOR SPHERICAL PARTICLES

In the case of a homogeneous sphere, the respective T-matrix elements in a given lth angular momentum channel are (see Eqs. (2.127) of [29])

$$T_{Al} = -\frac{m[xj_l(x)]'j_l(x_s) - j_l(x)[x_s j_l(x_s)]'}{m[xh_l(x)]'j_l(x_s) - h_l(x)[x_s j_l(x_s)]'}, \tag{A1}$$

where $m=\mu_s/\mu_h$ for TM mode ($A=M$), $m=\epsilon_s/\epsilon_h$ for TM mode ($A=E$), j_l and $h_l=j_l+in_l$ are the conventional spherical functions (see Section 10 of Ref. [30]), and primes denotes the derivative with respect to the argument. (The T-matrix elements correspond to the minus of the Mie expansion coefficients as given by Bohren and Huffman [4].) On using the asymptotic expansions (10.1.2) and (10.1.3) of [30] for j_l and n_l as $z\to 0$ up to the first three orders one arrives at

$$T_{E1} = i\frac{2x^3}{3}\frac{(\epsilon-1)\left[1-(\epsilon+1)\frac{x^2}{10}\right]}{\epsilon+2-(\epsilon-1)(\epsilon+10)\frac{x^2}{10}-i\frac{2x^3}{3}(\epsilon-1)}. \tag{A2}$$

The limiting expression [Eq. (A2)] for the T matrix coincides up to the order of x^2 with Eq. (45) of Kerker *et al.* [31]. The latter, however, does not comprise the k^3-dependent radiation reaction term. The asymptotic form [Eq. (A2)] can be recast as

$$T_{E1} = i\frac{2x^3}{3}\frac{\epsilon-1}{\epsilon+2-(6\epsilon-12)\frac{x^2}{10}-i\frac{2x^3}{3}(\epsilon-1)}, \tag{A3}$$

which facilitates a comparison with Eq. (4) resulting from the Meier and Wokaun prescription [3]. Meier and Wokaun [3] provided the following limiting expression (by correcting for a missing overall (2/3) prefactor, most probably due to a misprint in Eq. (5) of [3])

$$T_{E1} = i\frac{2x^3}{3}\frac{(\epsilon-1)\left(1-\frac{x^2}{10}\right)}{\epsilon+2-(7\epsilon-10)\frac{x^2}{10}-i\frac{2x^3}{3}(\epsilon-1)}. \tag{A4}$$

The latter can be shown to be equivalent to Eq. (A3) by multiplying both its numerator and its denominator by $f=1+x^2/10$. As a rule, by multiplying the numerator and denominator of Eq. (A3) by $f=1+(a\epsilon+b)x^2/10$, where a and b are arbitrary constants, one arrives at an equivalent expression, which, up to the order of x^3, differs from Eq. (A3) merely in different coefficients of the x^2 terms.

Note in passing that it does not make sense to convert the limiting expression [Eq. (A2)] into a power series in the size parameter x. The reason behind is that the respective expansion coefficients have $\epsilon+2$ in the denominator and become singular at the proximity of a SPR. (See, e.g., such an expansion for the Mie coefficient a_1 on p. 295 of [32], which is reproduced as Eq. (11) in [33].)

APPENDIX B: DIPOLAR SURFACE PLASMON RESONANCE POSITION IN THE EXACT LONG-WAVELENGTH LIMIT AND IN THE MEIER AND WORKAUN APPROXIMATION

The dipolar SPR position up to the order of x^2 is given by the following equation for the real part of $\epsilon=\epsilon'+i\epsilon''$ (see Section 12.1.1 of [4]):

$$\epsilon' \approx -2-\frac{12x^2}{5}. \tag{B1}$$

Contrary to that, Eqs. (4) and (58) imply that the real part of the denominator vanishes for

$$\epsilon' = -2 - 3x^2. \tag{B2}$$

Obviously, this differs from the result [Eq. (B1)] of Bohren and Huffman [4] by an additional redshift of the SPR position by $3x^2/5$.

It is worth remembering that all zeros of the T-matrix elements are *complex*. The distance of complex zeros to the real axis is a measure of a corresponding resonance linewidth. That a dipolar T-matrix element $T_{E1}=-a_1$ cannot have a zero for a real x even for a real ϵ is made transparent due to the presence of the radiative reaction term in Eq. (A2). Therefore, in a contradiction to the assertion in Section 12.1.1 of Ref. [4], the denominators of Mie's coefficients cannot vanish at real values of x. In the exact long-wavelength limit [Eq. (A2)], one finds for the dipolar SPR position, determined as a zero of the real part of the denominator of T_{E1} in Eq. (A2),

$$\epsilon' = -2 - \frac{24 + (\epsilon'')^2}{10}x^2 - \frac{2\epsilon''}{3}x^3 - \frac{6}{7}x^4. \tag{B3}$$

This formula can be viewed as an extension of the result [Eq. (B1)] of Bohren and Huffman [4] for absorbing particles. Indeed, the above formula reduces to Eq. (B1) for $\epsilon''=0$. An absorption ($\epsilon''>0$) provides an additional red shift to a SPR case compared with the $\epsilon''=0$ case. An additional consequence of Eq. (B3) with respect to the Bohren and Huffman [4] expression [Eq. (B1)] is that a temperature or light-intensity tuning of the SPR position may also be affected by changes in ϵ''.

APPENDIX C: UNITARITY

According to Eqs. (2.135), (2.137), and (2.138) of [29], one finds in the dipolar limit

$$\sigma_{\rm sca} \approx \frac{6\pi}{k^2}|T_{E1}|^2, \tag{C1}$$

$$\sigma_{\rm abs} \approx \frac{3\pi}{2k^2}(1 - |1 + 2T_{E1}|^2), \tag{C2}$$

$$\sigma_{\rm tot} \approx -\frac{6\pi}{k^2}\,{\rm Re}\,T_{E1}. \tag{C3}$$

(The above equations can easily be rephrased in terms of a particle polarizability on substituting $2ik^3\alpha/3$ for T_{E1}.) One then, somewhat misleadingly, refers to a *unitarity*, if the substitution of a given approximation to T_{E1} into the above equations yields $\sigma_{\rm tot}=\sigma_{\rm sca}+\sigma_{\rm abs}$.

It is straightforward to shown that any approximation that yields a *purely imaginary* T_{E1} [i.e., a *purely real* polarizability α, such as that given by the Rayleigh limit of Eq. (9) for real ϵ] violates the unitarity. Indeed, on using the defining equation for the S matrix, $S=1+2T$, one would arrive at

$$SS^* = (1 + 2T)(1 + 2T^*) = 1 + 4\,{\rm Re}\,T + 4|T|^2 = 1 + 4|T|^2 > 1, \tag{C4}$$

which is in contradiction with the exact bounds on a physical S matrix in potential scattering,

$$0 \leqslant SS^* \leqslant 1. \tag{C5}$$

In general, the bounds [Eq. (C5)] imply

$$-\frac{1}{4} - |T|^2 \leqslant {\rm Re}\,T \leqslant -|T|^2 \leqslant 0 \Rightarrow$$

$$\frac{2k^3}{3}|\alpha|^2 \leqslant {\rm Im}\,\alpha \leqslant \frac{2k^3}{3}|\alpha|^2 + \frac{3}{8k^3}, \tag{C6}$$

where the second bound follows from the first one on substituting $2ik^3\alpha/3$ for T.

APPENDIX D: IMPROPER INTEGRALS FOR POTENTIALS IN THE SOURCE REGION

Let us consider a function f that becomes infinite only at a single point P of the region V of integration. Then the integral

$$I = \int_V f{\rm d}V, \tag{D1}$$

is said to be *convergent*, or to exist, provided

$$\lim_{\delta\to 0}\int_{V-v} f{\rm d}V, \tag{D2}$$

exists, where v is a variable regular region subject to the sole restrictions that (i) it has the single point P in its interior, and (ii) its maximum chord length does not exceed δ (see Section VI.2. of [23]).

Kellogg's lemma (see lemma III on p. 148 of [23]): The integral

$$\int_V \frac{{\rm d}V}{r^\beta}, \quad 0 < \beta < 3, \tag{D3}$$

is *convergent*, and for all regular regions V of the same volume, it is greatest when V is a sphere about the singular point P.

APPENDIX E: COS$^{2N}\Theta$ QUADRATURE FORMULAS

For $\mathbf{E}_0$ polarized along the axis of rotational symmetry one finds in the case of a *prolate* spheroid

$$\int \frac{\cos^{2n}\theta}{2r}{\rm d}V = \pi a^2 \begin{cases} \dfrac{1}{e}\,{\rm arctanh}\,e & n=0 \\ \dfrac{1}{1-e^2}L_z & n=1 \\ \dfrac{1}{e^2}\left[\dfrac{L_z}{1-e^2} - \dfrac{1}{3}\right] & n=2 \end{cases}, \tag{E1}$$

whereas, for an *oblate* spheroid,

$$\int \frac{\cos^{2n}\theta}{2r}\mathrm{d}V = \pi a^2 \begin{cases} \dfrac{\sqrt{1-e^2}}{e}\arcsin e & n=0 \\ (1-e^2)L_z & n=1 \\ \dfrac{1-e^2}{3e^2}[1-3(1-e^2)L_z] & n=2 \end{cases}. \tag{E2}$$

For a sphere the above formulas reduce to

$$\int \frac{\cos^{2n}\theta}{2r}\mathrm{d}V = \frac{\pi a^2}{2n+1}. \tag{E3}$$

ACKNOWLEDGMENTS

I thank G.C. Schatz for providing me with a copy of [8], V. Šverak for calling my attention to [18] and for discussion, and an anonymous referee for a careful reading of the manuscript.

REFERENCES

1. T. S. Ahmadi, Z. L. Wang, T. C. Green, A. Henglein, and M. A. El-Sayed, "Shape-controlled synthesis of colloidal platinum nanoparticles," Science **272**, 1924–1926 (1996).
2. R. Jin, Y. Cao, C. A. Mirkin, K. L. Kelly, G. C. Schatz, and J. G. Zheng, "Photoinduced conversion of silver nanospheres to nanoprisms," Science **294**, 1901–1903 (2001).
3. M. Meier and A. Wokaun, "Enhanced fields on large metal particles: dynamic depolarization," Opt. Lett. **8**, 581–583 (1983).
4. C. F. Bohren and D. R. Huffman, *Absorption and Scattering of Light by Small Particles* (Wiley, 1998).
5. M. Meier, A. Wokaun, and P. F. Liao, "Enhanced fields on rough surfaces: dipolar interactions among particles of sizes exceeding the Rayleigh limit," J. Opt. Soc. Am. B **2**, 931–949 (1985).
6. A. Wokaun, "Surface-enhanced electromagnetic processes," in *Solid State Physics*, H. Ehrenreich, D. Turnbull, and F. Seitz, eds. (Academic, 1984), Vol. 38, pp. 223–294.
7. A. Wokaun, "Surface enhancement of optical fields mechanism and applications," Mol. Phys. **56**, 1–33 (1985).
8. E. J. Zeman and G. C. Schatz, "Electromagnetic theory calculations for spheroids: an accurate study of particle size dependence of SERS and hyper-Raman enhancements," in *Dynamics on Surfaces, Proceedings of the 17th Jerusalem Symposium on Quantum Chemistry and Biochemistry*, B. Pullman, ed. (Reidel, 1984), pp. 413–424.
9. E. J. Zeman and G. C. Schatz, "An accurate electromagnetic theory study of surface enhancement factors for silver, gold, copper, lithium, sodium, aluminum, gallium, indium, zinc, and cadmium," J. Phys. Chem. **91**, 634–643 (1987).
10. W.-H. Yang, G. C. Schatz, and R. P. van Duyne, "Discrete dipole approximation for calculating extinction and Raman intensities for small particles with arbitrary shapes," J. Chem. Phys. **103**, 869–875 (1995).
11. K. L. Kelly, E. Coronado, L. L. Zhao, and G. C. Schatz, "The optical properties of metal nanoparticles: the influence of size, shape, and dielectric environment," J. Phys. Chem. B **107**, 668–677 (2003).
12. P. Anger, P. Bharadwaj, and L. Novotny, "Enhancement and quenching of single-molecule fluorescence," Phys. Rev. Lett. **96**, 113002 (2006).
13. P. C. Waterman, "Symmetry, unitarity, and geometry in electromagnetic scattering," Phys. Rev. D **3**, 825–839 (1971).
14. M. I. Mishchenko, L. D. Travis, and A. A. Lacis, *Scattering, Absorption, and Emission of Light by Small Particles* (Cambridge U. Press, 2002).
15. A. Moroz, "Improvement of Mishchenko's *T*-matrix code for absorbing particles," Appl. Opt. **44**, 3604–3609 (2005).
16. J. J. Penninkhof, A. Moroz, A. Polman, and A. van Blaaderen, "Optical properties of spherical and oblate spheroidal gold shell colloids," J. Phys. Chem. C **112**, 4146–4150 (2008).
17. C. Pecharromán, J. Pérez-Juste, G. Mata-Osoro, L. M. Liz-Marzán, and P. Mulvaney, "Redshift of surface plasmon modes of small gold rods due to their atomic roughness and end-cap geometry," Phys. Rev. B **77**, 035418 (2008).
18. H. Kang and G. W. Milton, "Solutions to the Polya-Szego conjecture and the weak Eshelby conjecture," Arch. Ration. Mech. Anal. **188**, 93–116 (2008).
19. L. Landau and E. M. Lifschitz, *Electrodynamics of Continuous Media* (Pergamon, 1984).
20. J. D. Jackson, *Classical Electrodynamics*, 3rd ed. (Wiley, 1999).
21. A. F. Stevenson, "Electromagnetic scattering by an ellipsoid in the third approximation," J. Appl. Phys. **24**, 1143–1151 (1953).
22. M. Born and E. Wolf, *Principles of Optics*, 7th ed. (Cambridge U. Press, 2002).
23. O. D. Kellogg, *Foundations of Potential Theory* (Dover, 1953).
24. A. D. Yaghjian, "Electric dyadic Green's functions in the source region," Proc. IEEE **68**, 248–263 (1980).
25. A summary of formulas is given in supplementary material, which is available at http://www.wave-scattering.com/dplf-suppl.pdf
26. A. Moroz, "Electron mean-free path in a spherical shell geometry," J. Phys. Chem. C **112**, 10641–10652 (2008).
27. E. D. Palik, ed., *Handbook of Optical Constants of Solids* (Academic, 1985).
28. H. Kuwata, H. Tamaru, K. Esumi, and K. Miyano, "Resonant light scattering from metal nanoparticles: practical analysis beyond Rayleigh approximation," Appl. Phys. Lett. **83**, 4625–4627 (2003).
29. R. G. Newton, *Scattering Theory of Waves and Particles* (Springer, 1982).
30. M. Abramowitz and I. A. Stegun, *Handbook of Mathematical Functions* (Dover, 1973).
31. M. Kerker, D.-S. Wang, and H. Chew, "Surface enhanced Raman scattering (SERS) by molecules adsorbed at spherical particles: errata," Appl. Opt. **19**, 4159–4174 (1980).
32. R. Gans and H. Happel, "Zur Optik Kolloidaler Metallösungen," Ann. Phys. **29**, 277–300 (1909).
33. W. T. Doyle and A. Agarwal, "Optical extinction of metal spheres," J. Opt. Soc. Am. **55**, 305–308 (1965).